Chapter 5

New Organic Polymers for Solar Cells

Renat B. Salikhov, Yuliya N. Biglova and
Akhat G. Mustafin

Additional information is available at the end of the chapter

http://dx.doi.org/10.5772/intechopen.74164

Abstract

From the moment of conductive polyacetylene discovery, semiconducting polymers and other organic thin films and multilayers are important for a wide range of applications, including electronics, photovoltaics and sensors. The main idea of this chapter is the synthesis of new conjugated donor and acceptor polymers and development of organic solar cells on their basis. As donor polymers were used modified polyanilines (PANIs) and its dopants, as acceptor compounds - the fullerene C_{60} derivatives. Experimental prototypes of organic solar cells were obtained on the basis of binary donor-acceptor layers and bulk heterojunctions, consisting of novel polyaniline derivatives and fullerene-contained polymers. The current-voltage characteristics of solar cells were measured and the values of such parameters, such as open-circuit voltage, short-circuit current, fill factor and power conversion efficiency, were calculated. Comparison of parameters of the various types of organic solar cells was held.

Keywords: organic solar cell, polyaniline, fullerene-containing monomer and polymer, power conversion efficiency

1. Introduction

Organic materials with semiconductor properties have recently become the object of intensive research aimed at developing various elements of organic electronics: field-effect transistors, light-emitting diodes, memory cells, solar cells and sensors. After the opening of conductive polyacetylene [1], conjugated polymers are considered as a replacement for inorganic semiconductors. In the field of the development of organic solar cells (OSCs), real progress has been possible since the mid-1990s after the synthesis of conductive conjugated

polymers of the latest generation used for the production of modern light-emitting diodes and field-effect transistors.

Such polymers have excellent mechanical properties, the ability to process, a variety of forms and derivatives. They have a high absorption coefficient in the optical range, which allows their use in the form of ultra-thin films (about 100 nm thickness). The advantages mentioned above, as well as the possibility of depositing films from solutions at normal pressure onto flexible substrates of a large area, make it possible to manufacture an OSC using such relatively cheap methods as inkjet printing and stamping technique [2]. Despite these positive factors for the use of polymers, commercialization of the OSC is hampered both by relatively low-power conversion efficiency (PCE) of ~6–7% and by the need for protective encapsulation from environmental influences.

Almost all known types of organic photovoltaic cells can be divided into two main groups. The first group consists of batteries with a binary structure in which the photoactive components of the donor and acceptor types are deposited in separate layers. The second group includes batteries with a bulk heterojunction, in which there is only one photoactive layer, which is a mixture of a donor and an acceptor. In polymer solar cells, the active layers of the device must be located between two layers of conducting electrodes, one of which is transparent to incident light. Typically, for this purpose, a compound comprising indium tin oxide (ITO) coatings (a mixture of indium and tin oxides) applied to a glass or a flexible polymer substrate is used. In addition, the ITO layer is coated with a film of a conductive polymer used to transport holes—poly(3,4-ethylenedioxythiophene): poly(styrene sulfonate) (PEDOT: PSS). This film also serves to smoothen the surface of the ITO and prevent shunts from surface irregularities and to improve the efficiency of hole collection because of better matching of energy levels between the electrode yield and the highest occupied molecular orbital (HOMO) level of the donor polymer level. On the opposite side of the active layer, a metal electrode with a low work function is applied. In general, this is an aluminum electrode, which can be further modified by applying a thin layer (~1 nm) of LiF under it, which increases the efficiency of solar cells [3]. Lighting of such an element by sunlight is carried out from the side of a transparent glass or polymer substrate. Radiation is absorbed in the working polymer or composite layer, and electron-hole pairs (excitons) are generated, which then decay into electrons and holes collected on opposite electrodes. These processes are usually represented using energy diagrams (**Figure 1**).

The photovoltaic effect underlying the operation of the OSC consists of the generation of current carrier-electron and holes-in semiconductor materials when they are irradiated with light. The nature of the relatively low-efficient polymer OSCs in comparison with their inorganic analogs lies in the different mechanisms of photogeneration of free-charge carriers in such structures. When the inorganic semiconductors are illuminated by photons with an energy greater than the band gap, that is, the energy difference between the valence band and the conduction band, free charge carriers (electrons and holes) are generated, which are then separated by the pn junction of the solar cell.

In organic semiconductors, as a result of the absorption of photons, electrons from higher occupied molecular orbitals are excited to lower free molecular orbitals. An important difference

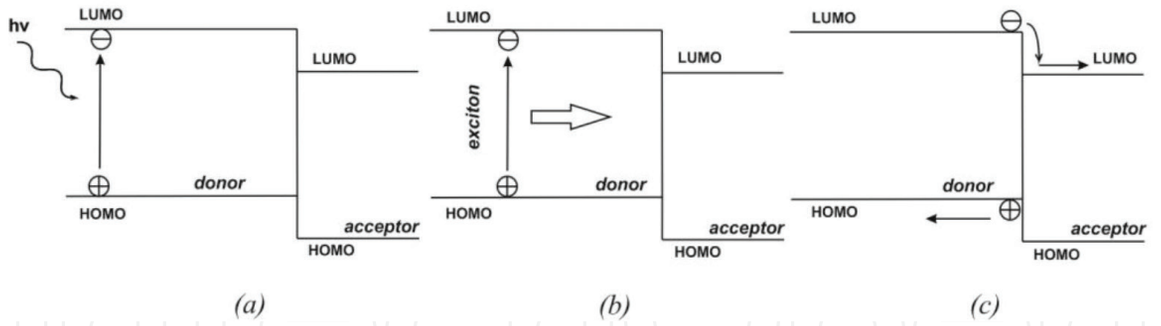

Figure 1. Energy diagrams of polymer binary system: (a) photon absorption, (b) exciton generation and (c) charge separation processes.

in the mechanisms of photogeneration in inorganic and organic materials is the fact that in free inorganic solar cells, free charge carriers are formed in the bulk of the material, whereas in OSC, as a result of their relatively low dielectric permittivity, such materials are bound by Coulomb interaction electron–hole pairs—excitons. To separate excitons and obtain free charges, an additional dissociation energy of excitons (binding energy) is required, which for different organic semiconductors is 0.2–1.0 eV. Generation of charges due to dissociation of excitons can be realized at the boundary of two organic semiconductors (donor and acceptor), that is, on a heterojunction.

By shifting the energy levels between the corresponding orbitals, organic materials can work as donors or electron acceptors. At the donor-acceptor interface, the process of charge transfer occurs, which leads to the appearance of holes in a material with a low ionization potential (donor) and electrons in a material with a high electron affinity (acceptor). These carriers are still connected by the Coulomb interaction but can be separated by an internal electric field (or built-in potential) of the solar cells, which is created in connection with the difference in the work function of the two different electrodes in the sandwich configuration of organic heterojunctions. Holes move through the donor material to the electrode with a high work function and electrons through the acceptor layer to the electrode with a low work function. The characteristic distance traveled by the exciton during its lifetime, that is, the diffusion length l_D, in organic semiconductors, is limited by a distance of about 10 nm due to their short lifetime and low mobility [4]. Obviously, only photons near the heterojunction plane, absorbed by the characteristic length l_D, contribute to the photocurrent. Only excitons that appear at distances comparable to l_D can effectively move toward the interface, thereby ensuring the generation of charge carriers. In practice, in the OSC with a binary structure, only a small part, about 0.01 absorbed photons, can contribute to the photocurrent.

A flat binary heterostructure consisting of two organic materials with shifted energy levels for the realization of the process of dissociation of an exciton into free charges was first demonstrated by Tang in 1986 [5]. It was shown that a photovoltaic effect occurs in a two-layer donor-acceptor system: metal phthalocyanine/perylene compound with a rather high efficiency. The coefficient of converting the energy of light into electrical energy was about 1%. An increase in light conversion efficiency of up to 2.5% was achieved in solar cells based on fullerene C_{60} as an acceptor material in combination with Cu or Zn phthalocyanines.

An important step in improving the efficiency of the OSC was the transition to a bulk heterojunction, which is realized by mixing donor and acceptor materials. The principle of operation of an OSC based on a bulk heterojunction is determined by the fundamental property of polymer materials, which consists of the striving for phase separation at the nanometer level. In the OSC of this type, the donor-acceptor interface, which penetrates the entire volume of the material, ensures the dissociation of excitons, as well as the transport of electrons and holes to the electrodes.

For the first time, solar batteries based on volumetric heterojunction obtained from solutions were reported in 1995. Since then, the number of publications in this field has started to grow exponentially, and the PCE has increased from 1 to 5% [6–10].

In the early years, poly [2-methoxy, 5-(20-ethyl-hexyloxy)-*p*-phenylene vinylene) (MEH-PPV)/C_{60} composites were later replaced by a better processed combination of poly [2-methoxy-5-(30,70-dimethyloctyloxy)-1,4-phenylene vinylene] (MDMO-PPV)/[6,6]-phenyl-$C_{61/71}$-butyric acid methyl ester ([60]PCBM or [70]PCBM). Because of the rather large band gap and low mobility of PPV-type polymers, the efficiency at best remained at 3%, and the general interest in this class of materials disappeared [11].

Recently, research efforts have focused on poly (alkyl-thiophenes) and in particular on poly (3-hexyl-thiophene) (P3HT). In 2002, the first encouraging results for P3HT: [60]PCBM solar cells at a 1: 3 weight ratio were published. At this time, the short-circuit current density was the largest ever observed in an organic solar cell (8.7 mA/cm^2) [12].

A mixture of P3HT: [60]PCBM was and remains dominant in studies of organic solar cells. Consider the material P3HT, which absorbs photons with a wavelength of less than 675 nm (energy of the band gap $Eg \approx 1.85$ eV). Assuming that in the P3HT: [60]PCBM mixture the polymer determines the optical gap of the composite, it is possible to calculate both the density of the absorbed photons and the absorbed power density. A typical spectrum of light incident on the Earth's surface is given by the standard AM1.5G. This standard defines parameters such as an integrated power density of 1000 W/m^2 (100 mW/cm^2), and an integrated photon flux of 4.31×10^{21} 1/s × m, distributed over a wide range of wavelengths (280—4000 nm) required for the characteristics of solar cells. The P3HT layer: [60]PCBM can absorb, at best, 27% of the available photons and 44.3% of the available power. Despite this, the real efficiency value for an organic solar cell based on P3HT: [60]PCBM does not exseed 5% [13].

To further increase the efficiency of solar cells, it is necessary to develop donor polymers that absorb light in an even longer wavelength region than P3HT, that is, the absorption boundary should lie at wavelengths greater than 700 nm. Such polymers should have a band gap (the difference in the energies of the lowest unoccupied molecular orbital [LUMO] and HOMO) of less than 2 eV.

The number of known donor polymers providing acceptable light conversion efficiency in photovoltaic cells is still small. In addition to the synthesis of new polymers, work is also under way to obtain new fullerene compounds for the purpose of using them instead of the [60]PCBM in photovoltaic cells.

In this regard, the aim of our chapter was the development of new acceptor components based on modified fullerene C_{60} and donors, based on soluble derivatives of polyaniline for use in organic solar cells.

2. Fullerene-containing polymers for organic solar cells

The inclusion of fullerene molecules into polymer chains as photo- and electroactive moieties (the subject of intense and competitive research in recent years) should lead to creating new materials with unique structural, electrochemical and photophysical properties. In recent years, many works that extensively use the metathesis strategy to obtain materials for photovoltaic cells have been published [14]. For example, the synthesis of vinyl-type polynorbornenes whose structure contains fragments of [60]PCBM, a conventional electron with drawing component of the active layer in organic photovoltaic cells, was proposed by Eo et al. [15]. Photovoltaic cells where the fullerene-containing copolymer acted as the n-type semiconductor in the active layer were developed based on these polymers. Also of interest are several works [16, 17] in which fullerene-containing monomers (FCMs) were subjected

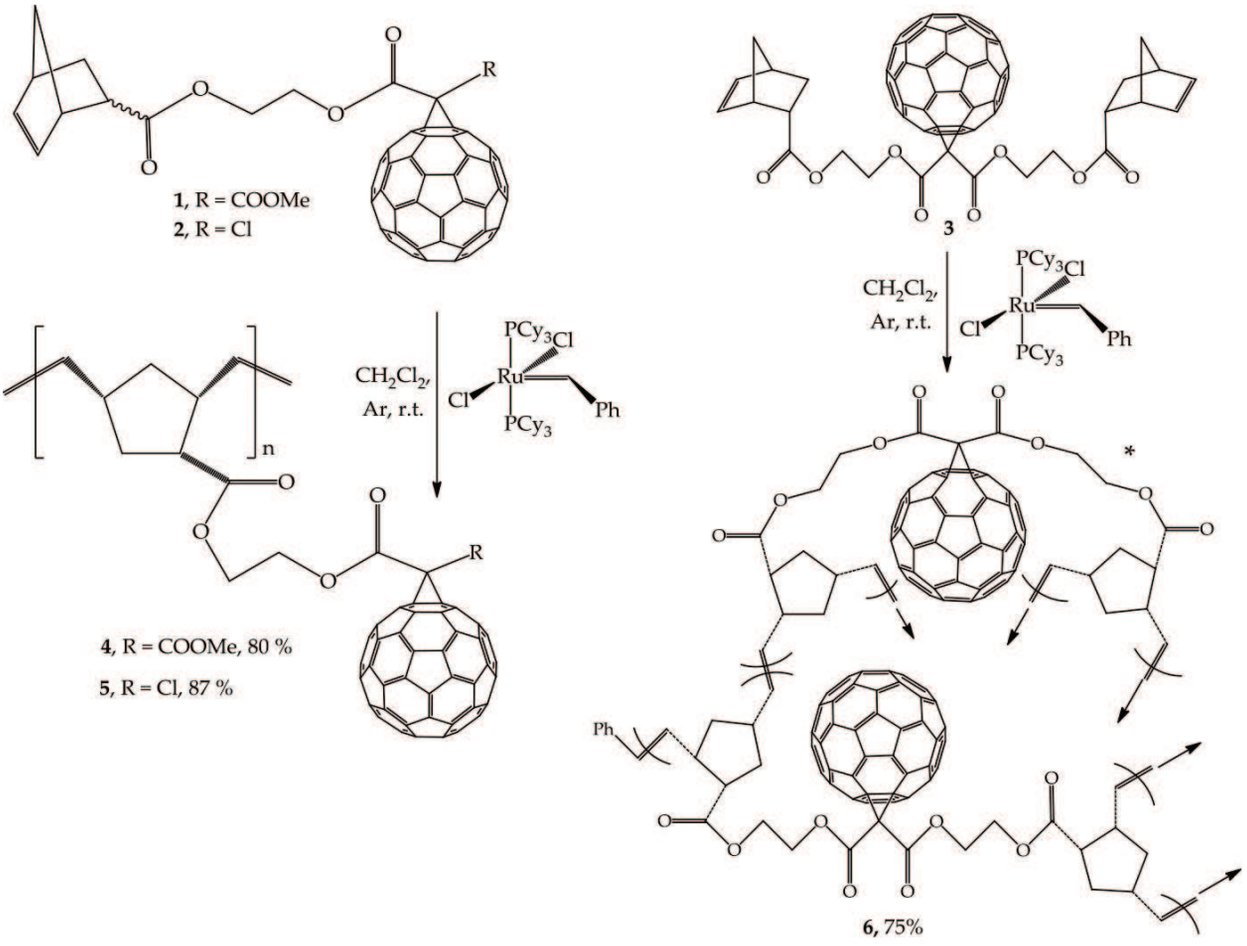

Figure 2. Ring-opening metathesis polymerization of fullerene-containing norbornene monomers.

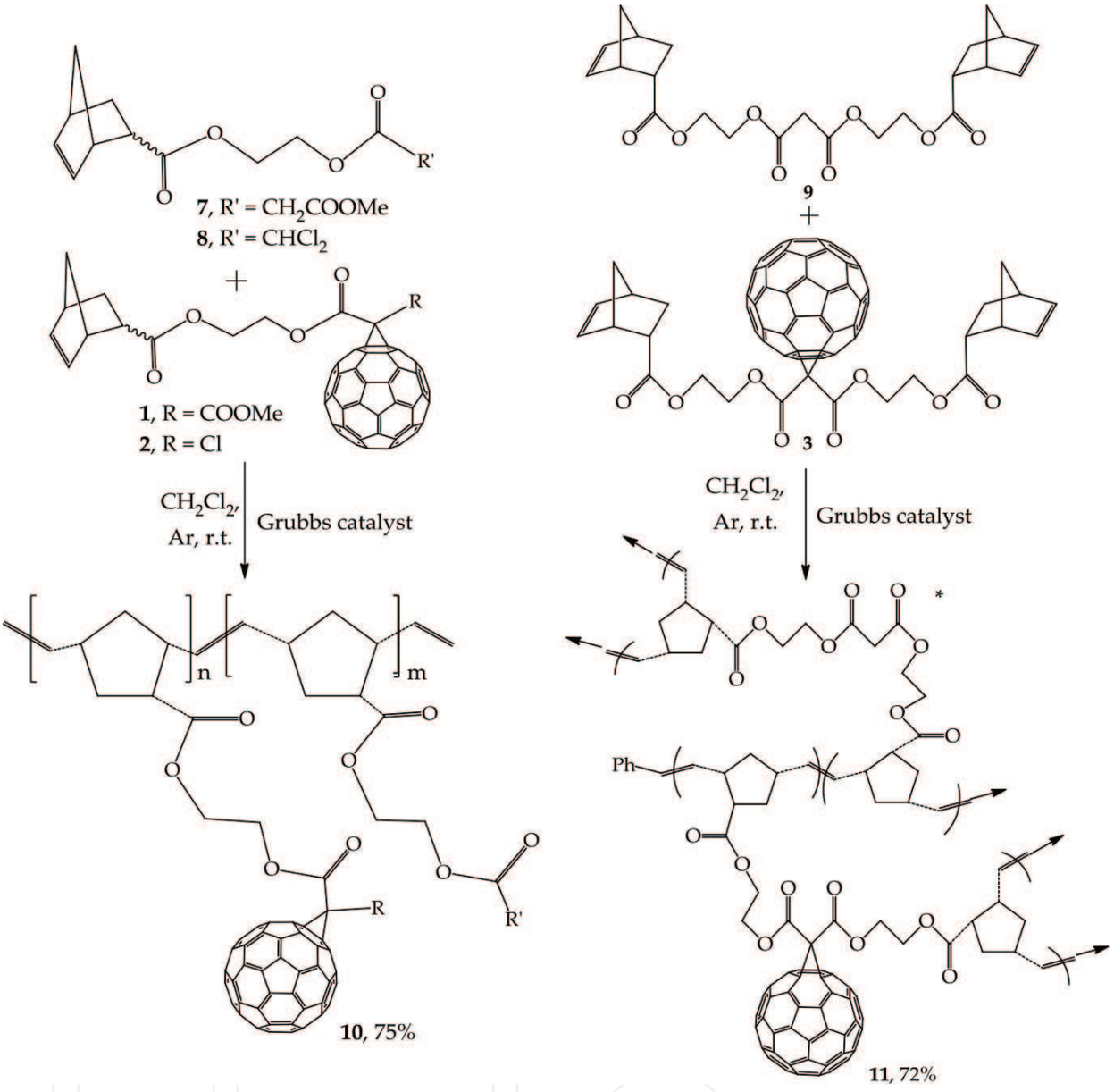

Figure 3. Ring-opening metathesis copolymerization of fullerene-containing norbornene monomers with related fullerene-free compounds.

to metathesis polymerization using a Grubbs catalyst and the products were tested in solar cells. This part of our work was devoted to synthesize new fullerene-containing polymers and copolymers from norbornene-type monomers in the presence of the first-generation Grubbs catalyst [$(PCy_3)_2Cl_2RuCHPh$].

Investigated in the work the fullerene-containing norbornene monomers include (**Figure 2**): {(1-methoxycarbonyl)-1-[(2-bicyclo[2.2.1]hept-5-en-2-yl)ethoxycarbonyl]-1,2-methano}-1,2-dihydro-C_{60}-fullerene (endo:exo = 6:1) **1** [18], {(1-chloro-1-[(2-bicyclo[2.2.1]hept-5-en-2-yl) ethoxycarbonyl]-1,2-methano}-1,2-dihydro-C_{60}-fullerene (endo) **2** [18] and bis[2-{[(2S*)-bicyclo[2.2.1]hept-5-en-2-yl]etoxycarbonyl}-1,2-dihydro-C_{60}-fullerene **3** [19].

The ring-opening metathesis polymerization of monomers **1–3** was carried out in the presence of the first-generation Grubbs catalyst at room temperature in CH_2Cl_2 in an argon atmosphere. In both cases, the consumption of the starting norbornenes **1–3** (TLC monitoring) and the precipitation of the polymers were observed for the first 3 h (**Figure 2**).

Synthesized homopolymers **4–6** were found to be insoluble in common organic solvents ($CHCl_3$, C_6H_6, PhMe, C_5H_4F and EtOAc), and to swell only partially in dimethyl sulfoxide, therefore, it seemed impossible to characterize their structures by spectral methods and to estimate their molecular weights.

Note that the results obtained do not contradict the other data available in this field. Some works showed that the incorporation of C_{60} fullerene into the polymer, in many cases, significantly deteriorates its solubility, which is due to the formation of intermolecular bonds involving polynorbornene fragments and C_{60} fullerene, as well as due to the restricted solubility of fullerene itself [14].

One of the possible ways to prepare soluble fullerene-containing polymers is involvement of fullerene monomers into copolymerization with highly soluble comonomers. This process is accompanied by the "effect of dilution" of rigid C_{60}-containing units due to the decrease in the concentration of fullerene molecules in the polymer chain, which has a favorable effect on the solubility of the final polymer. To reproduce this effect, norbornenes **1**, **2** and **3** were copolymerized with related fullerene-free compounds 2-[(bicyclo[2.2.1]hept-5-en-2-yl-carbonyl)oxy]ethylmethyl malonate (exo:endo = 6:1) **7** [18, 20], 2-[(2,2-dichloroacetyl)-oxy]ethyl bicyclo[2.2.1]hept5-ene-2-carboxylate (exo:endo = 6:1) **8** [18, 20] and bis[2-{[(2S*)-bicyclo[2.2.1] hept-5-en-2-yl carbonyl]oxy}ethyl)malonate **9** [19], respectively (**Figure 3**).

In all cases, the metathesis polymerization resulted in the formation of copolymers **10, 11** ($CHCl_3$, dimethylsulfoxide) soluble in some organic solvents with good degrees of conversion.

3. Soluble functionalized polyanilines

The development of a new generation of sensor devices is associated primarily with two conductive high-molecular compounds, namely, PANI and polypyrrole, which have been used in highly selective devices for the diagnosis of mixtures of gases and liquids, the so-called "electronic noses" and "electronic tongues" [21]. Biomedical studies of PANI are extremely promising. It has been shown that PANI can be used as a biocompatible electrode: electrical signals supplied to an in-vivo deposited polymer layer encourage the acceleration of tissue regeneration [22]. There is a wide range of already available and potentially possible applications of PANI. Nevertheless, the practical use of this material is limited by a number of serious problems. The first problem is related to the synthesis of PANI with reproducible properties. Samples of the polymer can contain a wide variety of aniline oxidation products with electrical conductivities that differ dozens of times. These products also differ in their spectral and magnetic characteristics and can have a fundamentally different morphology. Such an uncertainty leads to ambiguous results and requires a thorough investigation of the oxidative polymerization of aniline.

The second problem is related to the creation of materials for practical applications. A significant disadvantage of PANI is that it does not melt and is practically insoluble in conventional organic solvents. Therefore, PANI belongs to the category of non-recyclable materials. Furthermore, this polymer is a powder that has no adhesion to other materials.

Concerning this, it is obvious that the synthesis is a key process in the preparation of not only PANI but also PANI-based composites. Despite the apparent simplicity, the oxidative polymerization of aniline is a complex multistage reaction. The conventional procedure for chemical synthesis of PANI includes the oxidative polymerization of the monomer in an aqueous solution of an inorganic acid [23]. These conditions provide the formation of an unmeltable powder that is insoluble in the majority of available organic solvents. In order to eliminate the above disadvantages, PANI can be modified in different ways. An alternative version of the optimization of the performance characteristics of the polymer is the functionalization of the initial monomer rather than of the target product. In particular, the introduction of *o*-toluidine and *o*-anisidine (instead of aniline) into the polymerization process leads to the precipitation of high-molecular compounds soluble in organic solvents. Further, the homopolymer based on *o*-toluidine can be used in the design of electrochromic and photovoltaic devices. There are examples where the electrochemical polymerization of *o*-toluidine was performed with different solutions of acids used as electrolytes. In particular, Borole et al. [24] used sulfuric acid, *n*-toluenesulfonic acid, sulfamic acid and sulfosalicylic acid. A comparative analysis of the synthesized substances demonstrated that the maximum electrical conductivity was exhibited by a polymer soluble in the majority of conventional solvents, which was isolated with the participation of sulfonic acids. In a number of works, the method was proposed for the synthesis of high-molecular compounds with high electrical conductivity and good solubility by varying the ratio of comonomers (electrochemical polymerization). This made it possible to synthesize copolymers based on *o*-anisidine and *o*-toluidine [25]. It was noted that the most stable films are formed from a copolymer in which the content of pyrrole is more than 50% with respect to *o*-toluidine.

We carried out research identifying the most effective representatives and expanding the range of electrically conductive high-molecular compounds, primarily using functionalized aniline and researching the electrophysical and physicochemical properties of the target products.

Taking into account that the electrical conductivity of a high-molecular compound increases with the elongation of the conjugation chain, we turned to the development of the polymerization process of the functionalized derivative of aniline, rather than the aniline itself, and to the investigation of the physical and physicochemical properties of the obtained products.

The monomer used for the oxidative polymerization was the previously synthesized 2-(1-methyl-2-buten-1-yl)aniline **12** [26] with an alkenyl substituent that occupies the *o*-position of the aromatic ring and increases the conjugation chain. The diversity of the molecular structure, morphology and properties of the oxidation products of aniline is associated with the presence of the main reagents, namely, the monomer and the growing chain in unprotonated and protonated forms, as well as with the existence of two mechanisms of oxidation: the chain reaction of electrophilic substitution and the recombination of cation-radical centers. The contribution from the two reactions depends on the protonation state of the reagents and, consequently, on the pH of the reaction medium.

http://dx.doi.org/10.5772/intechopen.74164

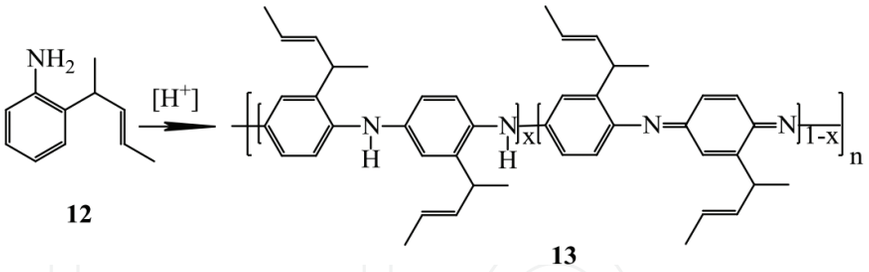

12 **13**

Figure 4. Homopolymerization of 2-(1-methyl-2-buten-1-yl)aniline **12.**

The homopolymerization of **12** was carried out by means of its oxidation, which resulted in the formation of a dark-green precipitate of polymer **13** in aqueous solutions of acids. The most frequently used oxidizing agent was ammonium persulfate. It is believed that the use of ammonium persulfate leads to the formation of a high molecular weight polymer with a high electrical conductivity.

The oxidation of aniline was performed in an acidic medium with hydrochloric acid at the pH = 0–2 according to the scheme shown in (**Figure 4**). Aniline-derivative copolymers **14–16** were synthesized in different molar ratios of *o*-toluidine and **12** (1:3. 1:1. 3:1, respectively) according to procedures similar to those used for the synthesis of homopolymer **13**. The yield of the copolymer was ~80%.

4. Charge transport in thin polymer films

Electronic conductivity of organic molecular compounds differs from that of metal and inorganic semiconductors such as silicon and germanium. The well-known band theory of crystal lattice is a good base to understand the conduction mechanism of crystalline molecular solids and conjugated and unconjugated polymers. At the same time, the applicability of the ideal elongated chain model to materials with a complicated morphology is naturally limited. Even within the frames of the idealized model, the inorganic conductors and semiconductors differ considerably from polymers. Besides, in polymers, the screening of interactions between charge carriers is less; electron–electron and electron–hole interactions play an important role causing considerable localization of electron states as compared with inorganic materials [27]. Absence of macroscopic ordering means inadequacy of band conduction model to describe electron conductivity of bulk polymer materials, though it can be used to a limited extent when studying the conduction process.

In amorphous layers of thin organic films the terms “conduction band” and “valence band” are usually replaced by the terms of the LUMO and the HOMO, respectively. The states’ density is mainly described quite satisfactorily by Gaussian distribution of localized molecular orbitals of individual molecules [28].

Depending on the size of barrier on the interface of electrode with polymer film, electric current flowing through the sample can be of injection type, that is, limited by space charge. In this case, one of the electrodes should be an ohmic one, that is, it should provide more charge

carriers in time unit than the sample is able to transport, not breaking Poisson's law. Otherwise, charge carrier transport across the interface will be limited by the barrier. The tunneling model of Fowler-Nordheim (FN) and Richardson-Schottky's (RSch) thermionic emission model are usually used to study injection in polymers in a rather strong electric field [29–31].

A thermal electron emission from hot metal is called thermionic emission. Electronic emission from metal contact into vacuum or dielectric conduction band by their thermal transportation through the potential barrier in electric field is called Schottky emission. Taking into account image forces in parabolic approximation, it is possible to get the Richardson-Schottky equation for current density [32]:

$$J = A \cdot T^2 \, exp\left[\frac{-e\left(\varphi_B - eF/4\pi\varepsilon\ \varepsilon_0\right)}{kT}\right], \tag{1}$$

where J is a current density, A is the Richardson constant, e is an electron charge, ϕ_B is a barrier height, F is a field density, ε is a dielectric permeability of a sample, ε_0 is the electric constant, k is the Boltzmann constant and T is temperature. An important assumption in RSch model is that electron can be taken out from the metal once it gets enough heat energy to cross the potential barrier which is formed by a superimposition of the external field and images forces.

According to the quantum theory, electron wave function within dielectric area located between two electrodes is different from zero. Wave function exponentially decreases with a distance into the barrier. If the barrier is very narrow, the probability to pass through the barrier for an electron has a finite value depending on the height and form of the potential barrier. Tunneling (auto-emission) can be observed in the case of a wide barrier if its effective thickness decreases under the influence of a strong electric field.

In the FN model image forces are disregarded and the tunneling of electrons from metal through a triangle barrier to free states of conduction area is considered. When the field intensity increases, the height and width of the potential barrier decreases to such an extent that a new physical effect appears and prevails: quantum mechanic tunneling of electron across the potential barrier. Current caused by the tunnel emission facilitated by a field is described by Fowler-Nordheim equation. In this case the current density can be described by the expression [33]:

$$J(F) = B\,F^2\,exp\left(-\frac{4\sqrt{2\,m_{eff}\left(e\,\varphi_B\right)^3}}{3\hbar eF}\right) \tag{2}$$

which is independent of temperature. Here, m_{eff} is the effective mass of a charge carrier in polymer and $\hbar$ is Planck's constant.

In spite of disadvantages of both FN and RSch concepts, they have been applied successfully to describe injections of a charge carrier in organic light-emitting diodes. For example, the FN model was applied to give reasonable values for the barrier height and to take into account independence of the temperature characteristic $J(F)$ in strong fields [34]. Thermionic emission prevails at the high temperatures and relatively low electric fields. Current caused by tunnel emission takes place at low temperatures and high values of electric fields.

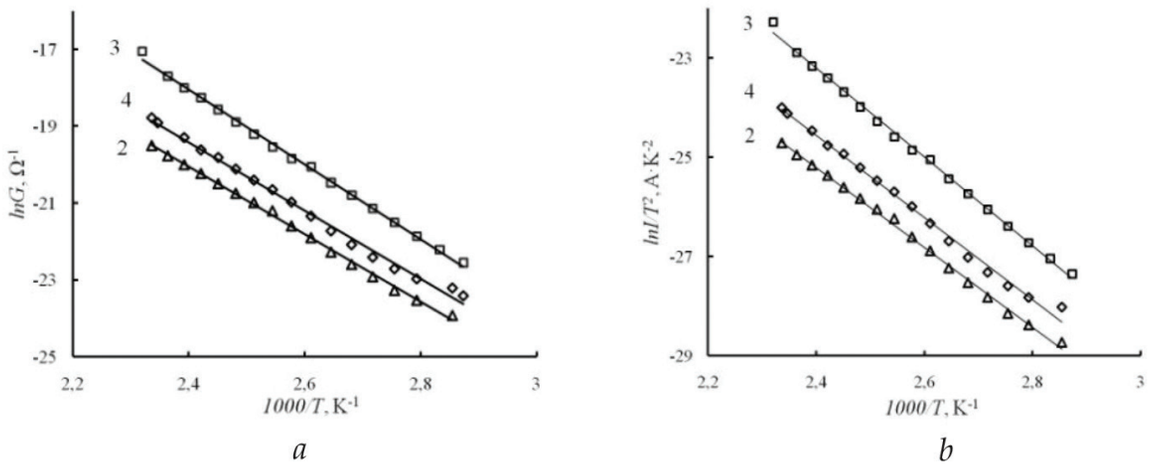

Figure 5. Dependences of (a) the electrical conductance and (b) I/T^2 on the inverse temperature for films of copolymers (o-toluidine with 2-(1-methyl-2-buten-1-yl)aniline) in different molar ratios: (2) 1:3, (3) 1:1, and (4) 3:1.

In Biglova et al.'s works [35], the temperature dependences of the electrical conductance were measured for films of different polyaniline forms. The measurements were carried out for soluble forms of the modified polyaniline homopolymer, that is, **12**, and its copolymers with o-toluidine in different molar ratios. The temperature measurements of the electrical conductance *G* of the polymer films in the range from 300 to 450 K demonstrated that the dependence of *G* on the temperature *T* has an exponential character:

$$G = G_0 \exp\left(-\frac{\Delta E}{2kT}\right). \tag{3}$$

In the *lnG – 1000/T* coordinates, the experimental points, within the limits of error, fall on a straight line (**Figure 5**). The quantity ΔE (**Table 1**) can be interpreted as the interval between HOMO and LUMO (an analog of the band gap) in semiconductor polymer films.

From the data presented in **Table 1**, it follows that the band gap varies from sample to sample and lies in the energy range from 1.39 to 1.66 eV. The dependence of the band gap on the molar ratio of the copolymers used for the preparation of thin films is an extremely important characteristic for their practical application in various electronic devices. The polymer compounds studied in this chapter can be used for the subsequent development of electronic devices similar to those based on inorganic $Ga_{1-x}Al_xAs$ heterostructures.

In order to understand how charge transfer occurs through the metal-polymer interface, we measured the temperature dependences of the current I flowing through the film structure. In the $lnI/T^2–1000/T$ coordinates, the graphical dependences, within the error of measurement, are well approximated by straight lines (**Figure 5**) in accordance with Eq. (1). The current density is defined as $J = I/S$, where *S* is the cross-sectional area of the film, which remains unchanged during the measurement. Therefore, the graphical dependences can be constructed using the values of the current flowing through the sample, rather than the values of current density. According to Eq. (1), the slopes of the straight-line sections are proportional to the Schottky barrier height φ_B. The results of the calculations are presented in **Table 1**.

№	E_{ox}^{1}, V	E_{red}^{1}, V	E_{HOMO}, eV*	E_{LUMO}, eV**	E_g, eV		φ_B, eV
					CVA	EP	
13	0.54	−1.07	−5.31	−3.73	1.61	1.55	0.71
14	0.49	−1.11	−5.29	−3.69	1.60	1.52	0.69
15	0.44	−1.13	−5.24	−3.67	1.57	1.68	0.77
16	0.29	−1.25	−5.09	−3.55	1.54	1.53	0.70

*$E_{HOMO} = -(E_{ox}^{1} + 4.8)$ (eV)
**$E_{LUMO} = -(E_{red}^{1} + 4.8)$ (eV)
CVA—cyclic voltammetry; EP—electrophysical measurements.

Table 1. Electrochemical characteristics of the synthesized polyaniline derivatives.

The analysis of the dependences obtained in this study allows the assumption that the main mechanism of charge carrier transfer through the interface between the metal substrate and the polymer film is the Schottky thermionic emission, which determines carrier transport in the temperature range from 300 to 450 K. This confirms the conclusion that the transfer of charge carriers through the metal-polymer interface occurs as a result of the above-barrier transport. In this case, the barrier height is determined by the difference between the work function of the metal and the electron affinity of the polymer. For example, the calculation according to the results of the electrophysical measurements for film samples of copolymers **15** gives the barrier height of 0.77 eV (**Table 1**). Taking into account that the work function of aluminum is 4.26 eV and the electron affinity of the polymer lies in the range from 3.5 to 3.6 eV, we obtain the barrier height ranging from 0.76 to 0.66 eV, that is, we have the value comparable to that calculated within the framework of the Schottky model. Since the field addition in Eq. (1) does not exceed 0.1 eV, it is ignored. Thus, the above calculations are further evidence in favor of the model of above-barrier transport at the metal-polymer interface.

The obtained values of HOMO and LUMO indicate that the polyanilines studied in our work can be used for the development of new organic solar cells [36, 37]. The short-circuit current of the photo-converter is closely related to the difference in the energy between the HOMO of the PANI (donor) and the LUMO of the acceptor. The most appropriate acceptor can be represented by a methanofullerene [38]. This difference also determines the open-circuit voltage. Moreover, the band gap of the donor determines the minimum energy or the maximum wavelength of the absorbed photons. For the effective absorption in the visible part of the solar spectrum, the band gap should be in the range from 1.4 to 1.5 eV.

Thus, the poly-2-(1-methyl-2-buten-1-yl)aniline/methanofullerene heterojunction, which is composed of newly synthesized compounds, is optimal for manufacturing a laboratory sample of a solar energy photoconverter.

5. Organic solar cells based on thin polymer films

The technique of formation of thin films of polyanilines and fullerene-containing polymers by vacuum deposition from a Knudsen effusion cell was used [36]. The length of the cylindrical

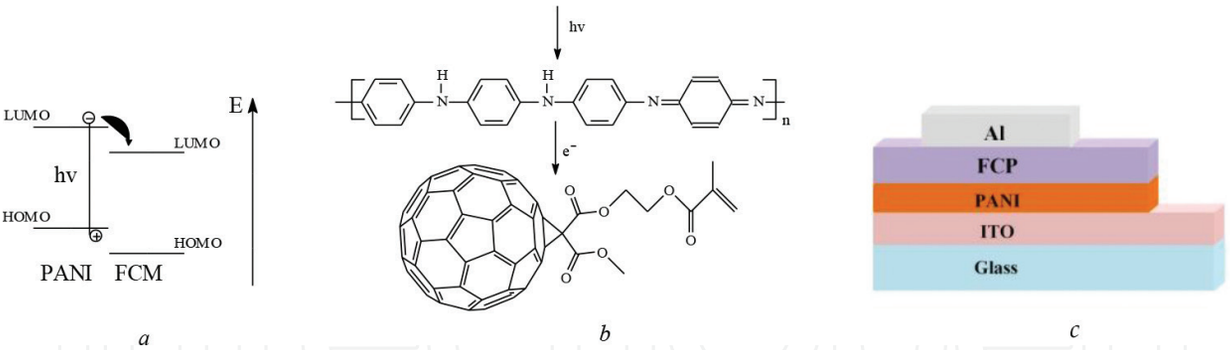

Figure 6. (a) An energy level diagram of the PANI/FCM system; (b) process of photon absorption and charge separation in this structure; (c) multilayer film structure of OSC.

cell was 25 mm, the internal diameter was 4 mm and the working temperature varied within the range 500–650 K. Thermal heating of fullerene-containing monomers (FCMs) during deposition led to their polymerization. Some thin films were formed by the spin coating technique from a solution of fullerene-containing monomers. All the obtained films were uniform in thickness, and their conductivity was about 0.1–1.0 mS/cm.

To increase the conductivity of polyaniline layers, the temperature conditions of deposition from the Knudsen cell were selected. The temperature range of 500–550 K proved to be the most optimal. In addition, protonation of the freshly prepared films in vapors of hydrochloric acid solution was carried out. For PANI films a conductivity value of 1.0 mS/cm was achieved as a result.

The surface condition and thickness of the deposited films were monitored on the basis of analysis of AFM images obtained by a NanoScan 3D. The thickness of photoactive layers varied and took on values within the range 100–200 nm. It should be noted that a too large thickness of the films leads to exciton recombination and reduces the efficiency of charge separation. On the contrary, the incident photon absorption and quantity of formed excitons decrease in overly thin films.

The organic solar cell test samples based on the donor-acceptor polymer systems described earlier were formed on a glass substrate with conductive and transparent ITO layers. Resistance of ITO layers was about of 10 Ω/□. For experimental structures of the OSC in this research the following organic substances were used: PANI, conventional fullerene and a novel synthesized monomer—monosubstituted methanofullerene derivative [38] (**Figure 6a** and **b**). The aluminum films fabricated by thermo-diffusion deposition in vacuum were applied as the upper electrode. **Figure 6c** presents the structure of the OSC in which thin films of PANI and fullerene-containing polymers were used as photoactive layers.

The current–voltage characteristics (CV characteristics) of all the prepared OSC samples were measured and the numerical values of such parameters such as open-circuit voltage, short-circuit current, filling factor and PCE were calculated on their basis. Measuring the CV characteristics of a photovoltaic cell is usually done by exposing it to steady-state illumination and a known temperature. The sun or a sunlight simulator can act as a light source. Estimations of the coefficient of efficiency were based on standard sun intensity $P_0 = 1000$ W/m^2 (AM 1.5 G conditions).

The values of these parameters for the various OSC experimental structures studied in this work appeared to be $J_{sc} = 0.6–1.8$ mA/cm^2 (short-circuit current), $V_{oc} = 0.6–0.8$ V (open-circuit voltage) and FF = 0.6–0.8 (filling factor). The highest values of PCE for the investigated

organic solar cells were about 2%. These values were obtained for the structures based on methanofullerene derivatives.

Thus, it was demonstrated that a combination of PANI with fullerene-containing polymers is very important for formation of OSC on the basis of binary donor-acceptor systems. The solar cells investigated here differ from earlier ones [39] that they can be fabricated on the flexible substrates.

6. Polymerizable methanofullerene as a buffer layer material for organic solar cells

In recent years, new combinations of semiconductor materials based on fullerene derivatives (n-type materials) and electron-conjugated polymers (p-type materials) are being actively developed all over the world. It is believed that the high efficiency of conversion of light in organic solar cells can be achieved only by using charge-selective buffer layers [40]. Usual materials for producing such layers are PEDOT: PSS and a number of inorganic oxides. Since PEDOT: PSS exhibits acidic properties, its use adversely affects the duration of the operation of solar cells. At the same time, the metal oxides in high oxidation states (MoO_3, V_2O_5 and WO_3) show oxidizing properties on the materials of the photoactive layer facilitating their breakage. The problem is observed even with relatively unreactive titanium dioxide TiO_2 [41].

The greatest prospects in terms of practical implementation have inverted configuration organic solar cells that do not contain high active metals and have significantly increased operational stability. However, the creation of these devices requires development of selective electron-transport buffer layers (ETL) based on semiconductor materials of n-type. We have fabricated inverted solar cells which ITO cathode, fullerene-containing buffer layer or ETL, photoactive layer, hole-transporting layer MoO_3 and Ag anode (**Figure 7**).

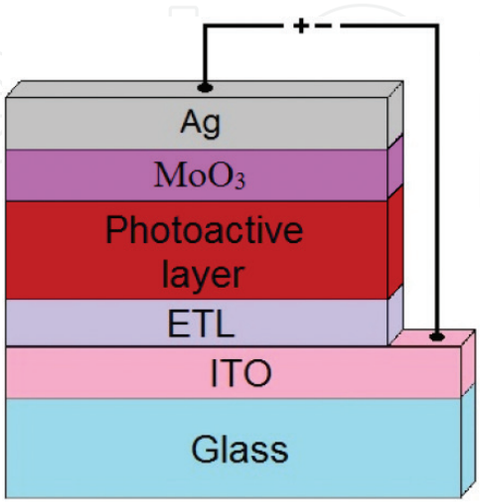

Figure 7. Schematic architecture of an inverted organic solar cell.

http://dx.doi.org/10.5772/intechopen.74164

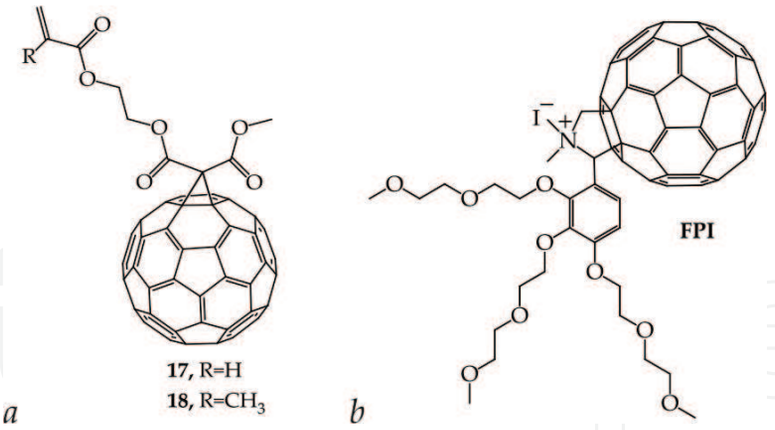

Figure 8. The molecular structures of the materials used to form ETL buffer layer of the devices.

The photoactive layer of organic solar cells was created on the basis of the traditional composites: the acceptor component [60]PCBM or [70]PCBM and conjugated polymer P3HT or poly[[9-(1-octylnonyl)-9H-carbazole-2,7-diyl]-2,5-thiophenediyl-2,1,3-benzothiadiazole-4,7-diyl-2,5-thiophenediyl] (PCDTBT).

In our study we propose usage of earlier synthesized {(1-methoxycarbonyl)-1-[2-(acryloyloxy) ethyloxycarbonyl]-1,2-methane}-1,2-dihydro-C_{60}-fullerene **17** [42] and {(1-methoxycarbonyl)-1-[2-(methacryloyloxy)ethyloxycarbonyl]-1,2-methane}-1,2-dihydro-C_{60}-fullerene **18** [38], containing in their structure unsaturated acrylate and methacrylate fragments (**Figure 8a**), taking into account that buffer layer must comply with the number of requirements. First, the forming method of its film must be straightforward and reasonably technological. Covering the ITO surface with methanofullerene solution in chlorobenzene, as it turned out, was a pretty simple buffer layer-forming approach, which did not request such processes as vacuum thermal evaporation and high-temperature annealing. Second, the formed film should be resistant to the effect of other solvents. Therefore, after laying one on the ITO surface we have had before us challenge of FCM insolubilization. For that reason solid-state radical polymerization has been conducted, which resulted in the creation of fullerene-containing polyacrylates and polymethacrylates.

At the first stage, the influence of the temperature of the heating of the buffer layer on the efficiency of light conversion in solar batteries was studied on the example of photoactive materials [60]PCBM and P3HT [43].

The current-voltage characteristics of organic solar cells (**Figure 9**) were measured under standard conditions using simulated solar light of AM 1.5 spectrum and intensity of 100 mW/cm^2 (calibrated Si diode used as reference) and a general-purpose source meter Keithley 400. The resulting parameters of the solar cells are given in **Table 2**.

The obtained data clearly demonstrate the positive effect on the characteristics of solar cell buffer layers produced by polymerization of fullerene derivatives **17** and **18**. Particularly exciting were high open-circuit voltages of 637–652 mV achieved by using polymerized **18** as a buffer layer. We would like to emphasize that such high voltages are very rare for the P3HT-[60]PCBM solar cells.

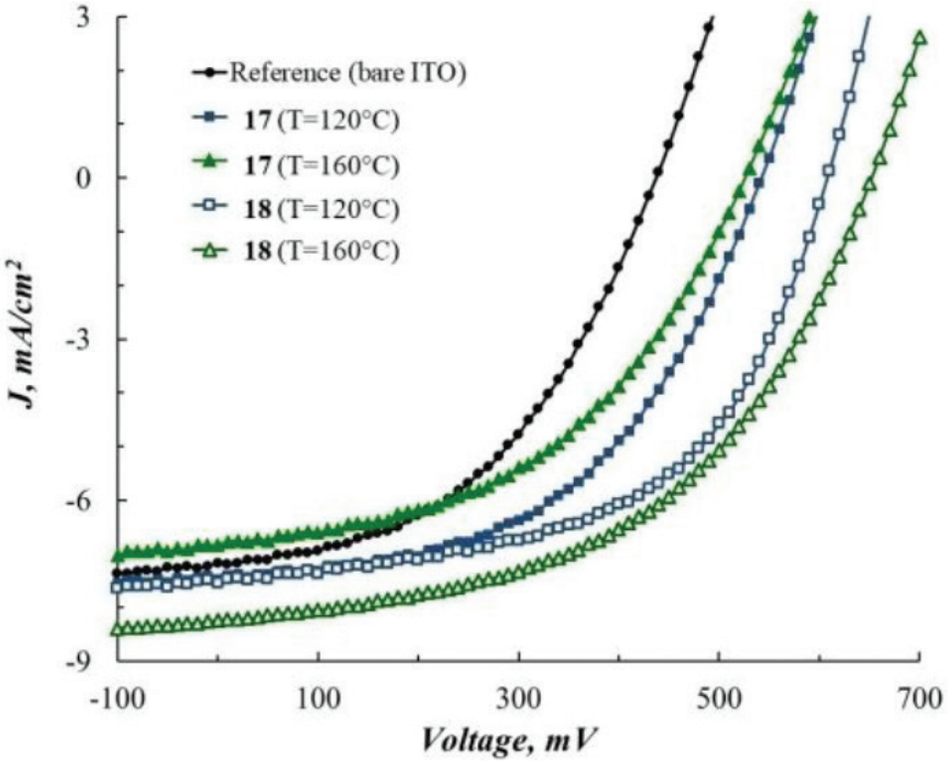

Figure 9. Selected CV characteristics of the inverted P3HT/[60]PCBM solar cells prepared on bare ITO (reference) and using buffer layers formed from polymerized **17** or **18.**

Buffer layer	$T_{(polymerization)}$, °C*	V_{oc}, mV	J_{sc}, mA/cm²	FF, %	PCE, %
—	—	437	7.2	46	1.5
17	120	542	7.5	50	2.0
	160	526	6.8	47	1.7
18	120	608	7.5	55	2.5
	160	652	8.2	50	2.7
	200	528	7.8	38	1.6

*annealing temperature of the buffer layer material **17** and **18** is provided.

Table 2. Parameters of the best inverted solar cells fabricated on bare ITO and using buffer layers formed from polymerized **17** and **18**.

At the second stage, we studied the impact of buffer layers on PCE and their forming methods on the substrate surface on the example of photoactive materials [70]PCBM and PCDTBT [44].

In recent years, a composite of PCDTBT: [70]PCBM was frequently used as an active layer in the standard organic solar cells OSC. This is based on the fact that the absorbance of [70] PCBM is much stronger than that of [60]PCBM and this property is very important for photovoltaic materials.

Four types of devices have been fabricated: without buffer layer (reference device) and with concentration of **17** in buffer layer 0.625, 1.25 and 2.5 mg/ml. Their current–voltage characteristic is given in **Table 3**.

Concentration 1, mg/ml	V_{oc}, mV	J_{sc}, mA/cm²	FF, %	PCE, %
—	446	8.7	36	1.4
0.625	618	11.1	39	2.7
1.250	587	9.1	39	2.1
2.500	620	8.6	36	1.8

Table 3. Current-voltage characteristics of inverted solar cells using different concentrations of **17**.

Table 3 shows that PCEs of the devices with ETL are higher than PCE of the reference device. The data in **Table 3** also marks a strong increase in open-circuit voltage at the implementation of 17, which is also noticeable, while other characteristics differ. The most probable explanation is that an n-type semiconductor facilitates photoelectric work function increase, and in turn Voc depends on the work function. A low FF highlights the need to conduct an additional optimization for active-layer forming to improve photovoltaic cell morphology, since FF depends on photoactive film morphology. Authors reported that FF can achieve 60–70% for the PCDTBT:[70]PCBM system. With this value of FF, our devices could achieve PCE of 4.5–4.8%. Thus highest performance has been demonstrated by the device with minimal concentration of 1. It is obvious that more optimal PCEs are arranged in the low-value areas of concentration. Properly, the less the concentration of the compound, the less the thickness of the formed layer. Presumably, further studies on increasing solar cells' efficiency will be held using small thickness of the buffer layer

At the third stage, we investigated the effect of the concentration of the buffer layer on the efficiency of light conversion in solar batteries as the example of photoactive materials [60]PCBM and P3HT or PCDTBT [45]. For this we propose ETL in inverted organic solar cells using a polymerizable mixture of acrylate derivative of [60]fullerene **17** and pyrrolidinofullerene

Photoactive materials	Concentration of 17 in the precursor solution, mg/mL*	V_{oc}, mV	J_{sc}, mA/cm²	FF, %	PCE, %
P3HT/[60]PCBM	—	409	6.9	46	1.3
	1.25	582	7.4	42	1.8
	2.50	591	6.5	43	1.7
	5.00	486	7.0	43	1.5
PCDTBT/[60]PCBM	—	585	6.6	42	1.6
	0.625	618	11.1	39	2.7
	1.25	677	8.3	54	3.0
	2.50	707	9.1	46	2.9
	5.00	712	7.5	41	2.2

*note that concentration of FPI in the precursor solutions was always 25 mol % with respect to the amount of **17.**

Table 4. Parameters of inverted P3HT/[60]PCBM and PCDTBT/[60]PCBM organic solar cells comprising **17** + FPI buffer layers as a function of **17** concentration in the precursor solution.

(FPI) (synthesized according to a published procedure [46]) (**Figure 8b**). The main parameters of the solar cells are given in **Table 4**.

The obtained results suggest that the electron-selective buffer layers based on the blends of the fullerene derivatives FPI and polymerizable **17** can be successfully used for fabricating inverted organic solar cells. The power conversion efficiencies for the inverted devices presented in this chapter were only 25–30% lower than the parameters of the standard-configuration organic solar cells. However, the latter contains reactive metal (calcium in our case) cathode that induces inherent instability leading to the rapid deterioration of the device parameters even under an inert atmosphere. Inverted devices showed lower open-circuit voltages (approximately by 100 mV) and fill factors as compared to the standard ones. Apparently, the electron work function of the fullerene-based buffer layer material is too high with respect to the conduction band (LUMO level) position of the n-type component of the photoactive layer ([60]PCBM).

Therefore, a Schottky-type barrier might be formed at the interface between the photoactive and the buffer layers. This might be a plausible reason for the observed reduction of the open-circuit voltages and fill factors of the inverted devices. To solve this problem, further research is needed with the aim to design some novel fullerene-based buffer-layer materials with lower-electron work functions.

7. Conclusion

In sum, the work carried out showed the advisability of application of new organic materials for solar cell development. A combination of PANI with fullerene-containing polymer was used for formation of OSC on the basis of binary donor-acceptor systems. The poly-2-(1-methyl-2-buten-1-yl)aniline/methanofullerene bulk heterojunction, which is composed of newly synthesized compounds, is optimal for the manufacturing of solar cells.

The potential use of polymerizable acrylate and methacrylate fullerene derivatives to form a buffer electron-selective charge-transport layer in inverted-configuration solar cells was demonstrated. Achieved light conversion efficiency indicates prospects of further development in this research. Optimization of technological conditions of the thin films fabrication and correct selection of the organic materials composition will provide higher values of OSC efficiency.

Author details

Renat B. Salikhov*, Yuliya N. Biglova and Akhat G. Mustafin

*Address all correspondence to: salikhovrb@ya.ru

Bashkir State University, Ufa, Russia

References

[1] Chiang CK, Fincher CR, Park YW Jr, Heeger AJ, Shirakawa H, Louis EJ, Gau SC, MacDiarmid AG. Electrical conductivity in doped polyacetylene. Physical Review Letters. 1977;**39**:1098-1101. DOI: 1010.1103/PhysRevLett.39.1098

[2] Shaheen SE, Ginley DS, Jabbour GE. Organic-based photovoltaics: Toward low-cost power generation. MRS Bulletin. 2005;**30**:10-19. https://www.calpoly.edu/~rechols/Phys422/MRS2005Intro.pdf

[3] Markov DE, Hummelen JC, Blom PWM, Sieval AB. Dynamics of exciton diffusion in poly(p-phenylene vinylene) fullerene heterostructures. Physical Review B. 2005;**72**:045216. DOI: doi.org/10.1103/PhysRevB.72.045216

[4] Dennler G, Lungenschmied C, Neugebauer H, Sariciftci NS, Labouret A. Flexible, conjugated polymer-fullerene-based bulk-heterojunction solar cells: Basics, encapsulation, and integration. Journal of Materials Research. 2005;**20**:3224-3233. DOI: Doi.org/10.1557/jmr.2005.0399

[5] Scharber MC, Muhlbacher D, Koppe M, Denk P, Waldauf C, Heeger AJ, Brabec CJ. Design rules for donors in bulk-heterojunction solar cells – Towards 10% energy-conversion efficiency. Advanced Materials. 2006;**18**:789-794. DOI: 10.1002/adma.200501717

[6] Kim JY, Kim SH, Lee HH, Lee K, Ma W, Gong X, Heeger AJ. New architecture for high-efficiency polymer photovoltaic cells using solution-based titanium oxide as an optical spacer. Advanced Materials. 2006;**18**:572-576. DOI: 10.1002/adma.200501825

[7] Peet J, Kim JY, Coates NE, Ma WL, Moses D, Heeger AJ, Bazan GC. Efficiency enhancement in low-bandgap polymer solar cells by processing with alkane dithiols. Nature Materials. 2007;**6**:497-500. DOI: 10.1038/nmat1928

[8] Kim JY, Lee K, Coates NE, Moses D, Nguyen TQ, Dante M, Heeger AJ. Efficient tandem polymer solar cells fabricated by all-solution processing. Science. 2007;**317**:222-225. DOI: 10.1126/science.1141711

[9] Gaudiana R, Brabec CJ. Organic materials: Fantastic plastic. Nature Photonics. 2008;**2**:287-289. DOI: 10.1038/nphoton.2008.69

[10] Green MA, Emery K, Hishikawa Y, Warta W. Solar cell efficiency tables. Progress in Photovoltaics: Research and Applications. 2008;**16**:61-67. DOI: 10.1002/pip.842

[11] Brabec CJ, Shaheen SE, Winder C, Sariciftci NS, Denk P. Effect of LiF/metal electrodes on the performance of plastic solar cells. Applied Physics Letters. 2002;**80**:1288. DOI: https://doi.org/10.1063/1.1446988

[12] Schilinsky P, Waldauf C, Brabec CJ. Recombination and loss analysis in polythiophene based bulk heterojunction photodetectors. Applied Physics Letters. 2002;**81**:3885. DOI: https://doi.org/10.1063/1.1521244

[13] Dennler G, Scharber MC, Brabec CJ. Polymer-fullerene bulk-heterojunction solar cells. Advanced Materials. 2009;**21**:1323-1338. DOI: 10.1002/adma.200801283

[14] Eo M, Han D, Park M, Hong M, Do Y, Yoo S, Lee M. Polynorbornenes with pendant PCBM as an acceptor for OPVs: Ring-opening metathesis versus vinyl-addition polymerization. European Polymer Journal. 2014;**5**:37-44. DOI: 10.1016/j.eurpolymj.2013.11.018

[15] Eo M, Lee S, Park M, Lee M, Yoo S, Do Y. Vinyl-type polynorbornenes with pendant PCBM: A novel acceptor for organic solar cells. Macromolecular Rapid Communications. 2012;**33**:1119-1125. DOI: 10.1002/marc.201200023

[16] Mehrotra S, Nigam A, Malhotra R. Effect of [60] fullerene on the radical polymerization of alkenes. Chemical Communications. 1997;**0**:463-464. DOI: 10.1039/A605555I. http://pubs.rsc.org/en/content/articlelanding/1997/cc/a605555i#!divAbstract

[17] Nayak P, Alva S, Yang K, Dhal P, Kumar J, Tripathy S. Comments on the analysis of copolymers of C_{60} with vinyl monomers obtained by free radical polymerization. Macromolecules. 1997;**30**:7351-7354. DOI: 10.1021/ma970318k

[18] Miftakhov M, Mikheev V, Torosyan S, Biglova Y, Gimalova F, Menshov V, Mustafin A. Fullerene containing norbornenes: Synthesis and ring-opening metathesis polymerization. Tetrahedron. 2014;**70**:8040-8046. DOI: 10.1016/j.tet.2014.08.039

[19] Biglova Y, Mikheev V, Torosyan S, Biglova R, Miftakhov M. Synthesis and ring-opening metathesis polymerization of fullerene-containing α, ω-bis-norbornenes. Mendeleev Communications. 2015;**25**:202-203. DOI: 10.1016/j.mencom.2015.05.014

[20] Biglova Y, Mustafin A, Torosyan S, Biglova R, Miftakhov M. Ring-opening metathesis polymerization (ROMP) of fullerene-containing monomers in the presence of a first-generation Grubbs catalyst. Kinetics and Catalysis. 2017;**58**:111-121. DOI: 10.1134/S0023158417020021

[21] Kondratiev V, Pogulaichenko N, Tolstopjatova E, Malev V. Hydrogen peroxide electroreduction on composite PEDOT films with included gold nanoparticles. Journal of Solid State Electrochem. 2011;**15**:2383-2393. DOI: 10.1007/s10008-011-1494-5

[22] Otero T, Martinez J, Arias-Pardilla J. Biomimetic electrochemistry from conducting polymers. A review: Artificial muscles, smart membranes, smart drug delivery and computer/neuron interfaces. Electrochimica Acta. 2012;**84**:112-128. DOI: 10.1016/j.electacta.2012.03.097

[23] Tarver J, Yoo J, Dennes T, Schwartz J, Loo Y. Polymer acid doped polyaniline is electrochemically stable beyond pH 9. Chemistry of Materials. 2009;**21**:280-286. DOI: 10.1021/cm802314h

[24] Borole D, Kapadi U, Mahulikar P, Hundiwale D. Electrochemical behaviour of polyaniline, poly (o-toluidine) and their copolymer in organic sulphonic acids. Materials Letters. 2004;**58**:3816-3822. DOI: 10.1016/j.matlet.2004.07.035

[25] Borole D, Kapadi U, Mahulikar P, Hundiwale D. Electrochemical synthesis and characterization of conducting copolymer: Poly (o-aniline-co-o-toluidine). Materials Letters. 2006;**60**:2447-2452. DOI: 10.1016/j.matlet.2006.01.014

[26] Abdrakhmanov I, Mustafin A, Sharafutdinov V. Claisen Rearrangement in Aromatic Amines. Gilem; 2014. p. 168. DOI: 10.1002/chin.198913176

[27] Hadziioannou G, Hutten PF. Semiconducting Polymers. Chemistry, Physics and Engineering. Wiley-VCH Verlag GmbH; 2000. p. 613. DOI: 10.1002/3527602186.fmatter

[28] Schmechel R, Seggern H. Electronic traps in organic transport layers. Physica Status Solidi. 2004;**201**:1215-1235. DOI: 10.1002/pssa.200404343

[29] Gadiev RM, Lachinov AN, Salikhov RB, Rakhmeev RG, Kornilov VM, Yusupov AR. The conducting polymer/polymer interface. Applied Physics Letters. 2011:98-173305. DOI: https://doi.org/10.1063/1.3584135

[30] Salikhov RB, Bunakov AA, Lachinov AN. Charge transfer in thin polymer films of polyarylenephthalides. Physics of the Solid State. 2007;**49**:185-188. https://link.springer.com/article/10.1134/S1063783407010295

[31] Salikhov RB, Rakhmeev RG, Lachinov AN. Transport layer at the boundary of two polymer films. Technical Physics Letters. 2008;**34**:495-497. https://link.springer.com / article/10.1134/S1063785008060138

[32] Sze SM. Physics of Semiconductor Devices. 2nd ed. New York: J.Wiley; 2002. 564 p

[33] Fowler RH, Nordheim L. Electron emission in intense electric fields. Proceedings of the Royal Society of London A. 1928;**119**:173-181. DOI: 10.1098/rspa.1928.0091

[34] Parker ID. Carrier tunneling and device characteristics in polymer light-emitting diodes. Journal of Applied Physics. 1994;**75**:1656. DOI: 10.1063/1.356350

[35] Biglova YN, Salikhov RB, Abdrakhmanov IB, Salikhov TR, Safargalin IN, Mustafin AG. Preparation and investigation of soluble functionalized polyanilines. Physics of the Solid State. 2017;**59**:1253-1259. DOI: 10.1134/S106378341706004X

[36] Salikhov RB, Biglova YN, Yumaguzin YM, Salikhov TR, Miftakhov MS, Mustafin AG. Solar-energy photoconverters based on thin films of organic materials. Technical Physics Letters. 2013;**39**:854-857. https://link.springer.com/article/10.1134/S1063785013100106

[37] Salikhov RB, Biglova YN, Salikhov TR, Yumaguzin YM. New polymers for organic solar cells. Journal of Nanoelectronics and Optoelectronics. 2015;**9**:792-794. https://doi.org/10.1166/jno.2014.1679

[38] Torosyan S, Biglova Y, Mikheev V, Khalitova Z, Gimalova F, Miftakhov M. Synthesis of fullerene-containing methacrylates. Mendeleev Communications. 2012;**22**:199-200. DOI: 10.1016/j.mencom.2012.06.009

[39] Wang W, Schiff EA. Polyaniline on crystalline silicon heterojunction solar cells. Applied Physics Letters. 2007;**91**:133504. DOI: 10.1063/1.2789785

[40] Yang P, Chen S, Liu Y, Xiao Z, Ding L. A pyridine-functionalized pyrazolinofullerene used as a buffer layer in polymer solar cells. Physical Chemistry Chemical Physics. 2013;**15**:17076-17078. DOI: 10.1039/C3CP53426J

[41] Kim D, Jeong M, Seo H, Kim Y. Oxidation behavior of P3HT layers on bare and TiO_2-covered ZnO ripple structures evaluated by photoelectron spectroscopy. Physical Chemistry Chemical Physics. 2015;**17**:599-604. DOI: 10.1039/C4CP03665D

[42] Torosyan S, Biglova Y, Mikheev V, Gimalova F, Mustafin A, Miftakhov M. New monomers for fullerene-containing polymers. Russian Journal of Organic Chemistry. 2014;**50**:179-182. DOI: 10.1134/s1070428014020067

[43] Biglova Y, Susarova D, Akbulatov A, Mustafin A, Troshin P, Miftakhov M. Acrylate and methacrylate derivatives of fullerenes as electron-selective buffer layer materials for inverted organic solar cells. Mendeleev Communications. 2015;**25**:348-349. DOI: 10.1016/j.mencom.2015.09.010

[44] Biglova Y, Akbylatov A, Torosyan S, Susarova D, Mustafin A, Miftakhov M. New methanofullerene as a buffer layer in organic solar cells. Physica B: Condensed Matter. 2015;**458**:114-116. DOI: 10.1016/j.physb.2014.11.025

[45] Biglova Y, Susarova D, Akbulatov A, Mumyatov A, Troshin P. Polymerizable methanofullerene bearing pendant acrylic group as a buffer layer material for inverted organic solar cells. Mendeleev Communications. 2015;**25**:473-475. DOI: 10.1016/j.mencom.2015.11.026

[46] Li C, Chueh C, Yip H, O'Malley K, Chen W, Jen A. Effective interfacial layer to enhance efficiency of polymer solar cells via solution-processed fullerene-surfactants. Journal of Materials Chemistry. 2012;**22**:8574-8578. DOI: 10.1039/c2jm30755c